



## ANALYSIS OF IMPACTING FACTORS FOR SOIL-CEMENT COLUMN COMBINED HIGH STRENGTH GEOGRID

Nguyen Thai Linh, Nguyen Duc Manh, Nguyen Hai Ha

University of Transport and Communications, No 3 Cau Giay Street, Hanoi, Vietnam

### ARTICLE INFO

TYPE: Research Article

Received: 5/10/2020

Revised: 30/10/2020

Accepted: 6/11/2020

Published online: 25/01/2021

<https://doi.org/10.47869/tcsj.72.1.2>

\* *Corresponding author*

Email: [thailinhdkt@utc.edu.vn](mailto:thailinhdkt@utc.edu.vn)

**Abstract.** Soil-cement column combined with geogrid on top or Geogrid Reinforced Pile Supported (GRPS) is used to construct the structures on soft ground. Because of its high tensile capacity, the geogrid is spread on the top of the soil-cement column to form a soft transmission layer, increasing the capacity transferred to the columns, reducing a part of the load transmitted to the soft soil between the columns. The numerical analysis results of the GRPS with a high strength geogrid showed four major factors affecting transmission the efficacy of the column ( $E_f$ ) and the tensile force of the geogrid including effective vertical load ( $\sigma_v'$ ); the ratio of the distance between the columns and the column's diameter ( $s/D$ ); the ratio of the elastic modulus of the soil-cement column to the deformation modulus of soil ( $E_c/E_s$ ); the tensile stiffness of the geogrid ( $J$ ). The efficacy of the column ( $E_f$ ) increases rapidly with an increase in effective vertical load ( $\sigma_v'$ ) from 0.23 to 0.44. In contrast, the transmission efficiency ( $E_f$ ) decreases from 0.60 to 0.37 when  $s/D$  increased. When the ratio  $E_c/E_s > 150$  and  $J > 8000$  kN/m, the tensile force of the geogrid tends not to change much.

**Keywords:** soil cement-column, Geogrid-reinforced, efficient of load transmission numerical model.

© 2021 University of Transport and Communications

### 1. INTRODUCTION

Geosynthetic-reinforced and pile-supported (GRPS) embankment have been successfully used in soft soil treatment [1]. The reinforced earth platform includes one or more layers of geogrid (geosynthetic) at the base of the embankment and on top columns. With this method,

the weight of the embankment and the surcharge are largely transferred onto the columns so that the soft soil between the columns carry less load and the embankment settlement is reduced [2].

Soil arching and membrane effect are identified as the key load transfer mechanisms. Soil arching develops above the geogrid-reinforced fill platform when differential settlement occurs between columns and the surrounding soil. Meanwhile, the membrane effect is expressed through the tensile force of the geogrid.

Many studies consider the mechanisms of load transfer of a GRPS system to be a combination of soil arching, tensioned membrane or stiffened platform effects, and the relative stiffness effects between the piles and the soil. However, the behavior of GRPS embankment systems is not yet fully understood, especially when the geosynthetic reinforcement layer is the high strength geogrid. A numerical study was conducted to investigate the stress distributions and the transfer behavior of the high strength geogrid-reinforced embankments on soil-cement columns.

## 2. EVALUATION PARAMETERS OF THE LOAD TRANSFER MECHANISM OF GRPS EMBANKMENTS

In the working of the soil-cement column combined with geogrid, the efficacy of the column is the basic parameter to evaluate the effectiveness of the soil arching [3], [4]. It can be expressed as:

$$E_f = \frac{P}{s^2 \cdot \gamma \cdot H} \quad (1)$$

Where P is the total load carried by column (kN),  $\gamma$  is the unit weight of the embankment fill material (kN/m<sup>3</sup>), H is the embankment height (m) and s is the spacing between columns (m).

The tensile force T of the geogrid is an evaluation parameter of the membrane effect in the GRPS system [5]–[7]. The tensile force T is determined as follows:

$$T = J \cdot \varepsilon \quad (kN/m) \quad (2)$$

Where J is the stiffness of the geogrid (kN/m);  $\varepsilon$  - the strain of the geogrid.

## 3. NUMERICAL MODELING AND ANALYSIS

Embankment geometry and GRPS-reinforced ground for the benchmark case are shown in Fig.1. Due to symmetry, only half of the embankment was modeled to save computation time. The commercial FE package PLAXIS 3D was used for the FE modeling. The model shown in Fig.1 consists of 28105 nodes and 21650 elements. The thickness of the model is 6m to contains two rows of columns in the x-direction.

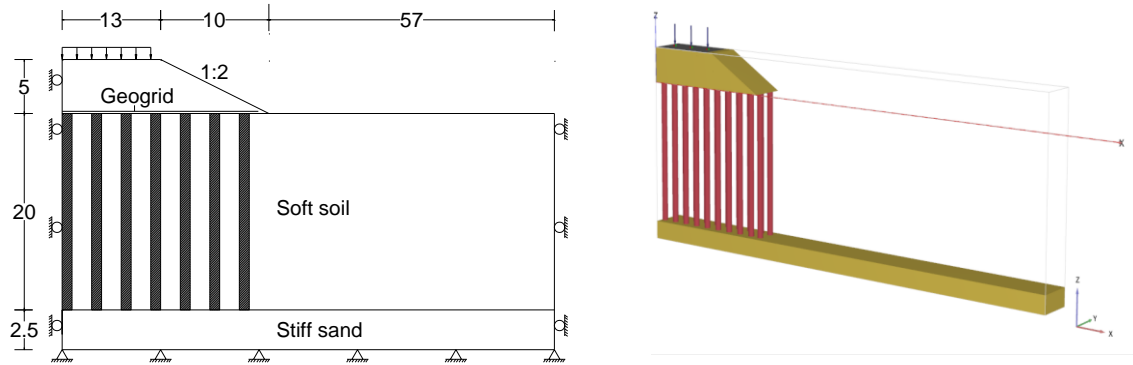


Figure. 1. Dimensions and boundary conditions in the numerical model.

As seen in this figure, a 13 m wide embankment having side slope 1V: 2H is constructed on 20 m soft clay underlying by a rigid layer. The number of soil-cement columns is 14 (two rows) and the diameter of the soil-cement column for all analyses was kept 1.0 m. The boundary effect was investigated to extend the right boundary successively up to 57 m from the toe of the embankment. It was found that it would be sufficient to eliminate the boundary effect if the boundary was set at 57 m from the toe. The bottom boundary is fixed in both horizontal and vertical directions and two side boundaries are fixed in the horizontal direction but free in the vertical direction.

For simplicity, the following elements were modeled as linearly elastic-perfectly plastic materials using the Mohr-Coulomb failure criteria: the soil-cement column, the soft soil, the firm soil, and the embankment fill [1], [5], [8]. This case study demonstrates that the numerical method with a simple linear-elastic perfectly plastic model can predict the efficacy of the column and the tensile stiffness of the geogrid within a geogrid-reinforced embankment over soil-cement columns reasonably well [1],[9].

Geogrid elements were used to model the geogrid layer. The interface between the soil, the geogrid and the columns were assumed to be fully bonded for simplicity purposes. The elastic modulus of soil-cement columns should be  $100q_u$  [4], [10], [11] (where  $q_u$  is unconfined compression strength). The construction process was simulated by adding the embankment fill in successive layers of 1.0 m height. The material properties used in the numerical analysis are tabulated in Table 1.

Table 1. Material Properties used in the Numerical Analysis Material.

	<b>E (MPa)</b>	<b><math>\nu</math></b>	<b><math>\gamma</math> (kN/m<sup>3</sup>)</b>	<b><math>c'</math> (kN/m<sup>2</sup>)</b>	<b><math>\phi</math> (°)</b>
<b>Sand fill</b>	10	0.3	18.5	0	35
<b>Soft soil</b>	1	0.35	18.0	8.5	7
<b>DCM</b>	150	0.3	18.5	750	0
<b>Geogrid</b>	<b>J = 8000 kN/m.</b>				

Note:  $E$  = elastic modulus,  $\nu$  = Poisson's ratio,  $\gamma$  = unit weight,  $c'$  = effective cohesion,  $\phi$  = effective friction angle,  $J$  = tensile stiffness of geogrid.

To investigate the stress behavior of the GRPS embankments, four major influencing factors were considered: (1) including effective vertical load (ranging from 18.5 kPa to 105 kPa); (2) the ratio of the distance between the columns and the column's diameter ( $s/D = 2.0, 2.5, 3.0, 3.5$ ); (3) the ratio of the elastic modulus of the soil-cement column to the deformation modulus of soil ( $E_c/E_s = 50, 100, 150, 200, 250$ ); (4) the tensile stiffness of the geogrid ( $J = 2000 \text{ kN/m}, 4000 \text{ kN/m}, 6000 \text{ kN/m}, 8000 \text{ kN/m}$  and  $10000 \text{ kN/m}$ ).

### Influence of the effective vertical load

Fig.2 presents the influence of the effective vertical load on the efficacy of the column and the tensile force of the geogrid. It is shown that the efficacy of the column increases with the growth of the effective vertical load. Besides, the vertical load is the main factor that increases the tensile force of the geogrid.

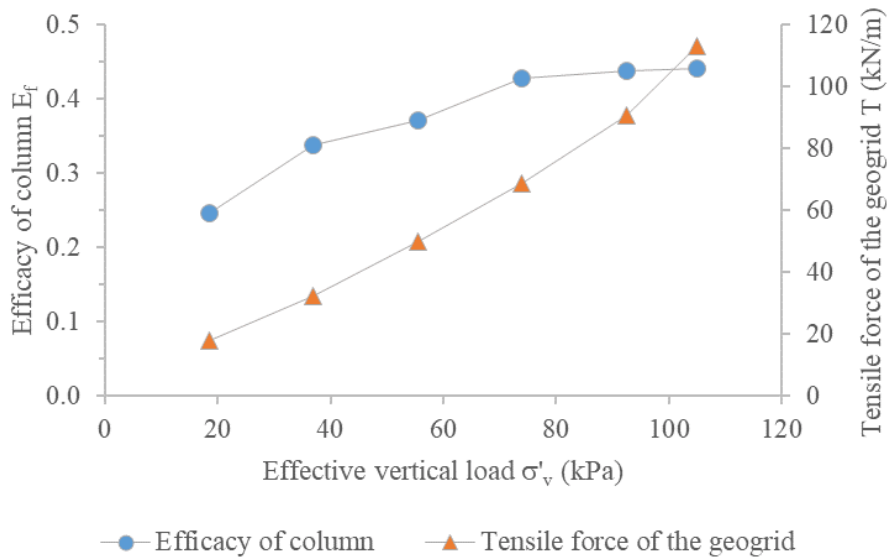


Figure 2. Influence of the effective vertical load.

### Influence of the spacing of the columns

It is shown from Fig.3 that the efficacy of the column decreases with an increase in the spacing of the columns. Meanwhile, the tensile force of the geogrid is larger when the distance between the columns is greater. This is because due to with increasing  $s/D$ , increasing differential settlement between columns and soft soil, generally increases the degree of arching (transferring more embankment load to columns) and the tensile force of the geogrid. However, that increase is not sufficient to reverse the lowering of efficiency coefficient of columns with increasing  $s$ . But until the ratio  $s/D > 3$ , the tensile force tends to be constant due to which stable soil arching was formed.

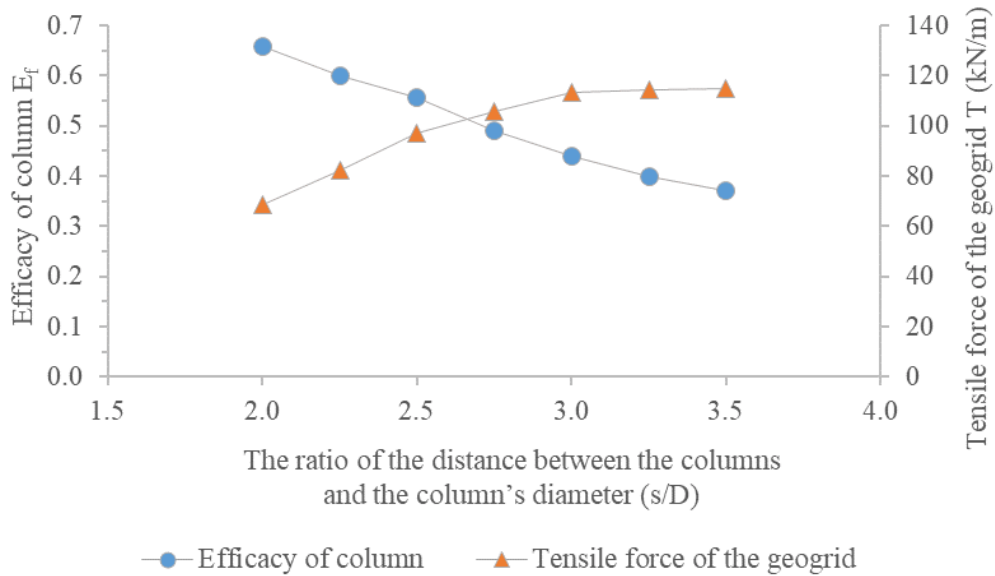


Figure 3. Influence of the ratio of the distance between the columns and the column's diameter.

**Influence of the ratio of the elastic modulus of the column to the deformation modulus of soil**

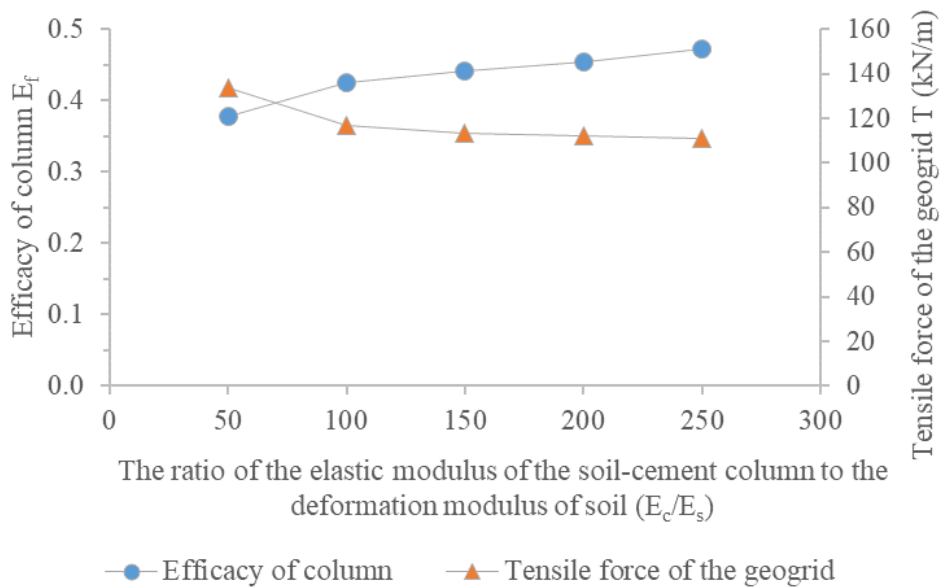


Figure 4. Influence of the ratio of the elastic modulus of the soil-cement column to the deformation modulus of soil.

Fig.4 presents the influence of the ratio of the elastic modulus of the soil-cement column to the deformation modulus of soil on the efficacy of the column. It is shown that the stress on the columns increases with the growth of the elastic modulus of the column. This is because due to the geogrid reinforcement, columns were stiff enough as compared to surrounding soft clay due to which stable soil arching was formed, the change of the ratio of the elastic modulus does not appear to have an influence on the tensile force of the geogrid.

### Influence of the Tensile Stiffness of the geogrid

Fig. 5 presents the influence of the tensile stiffness of the geogrid on the tensile force of the geogrid. It is shown from Fig.5 that with increasing  $J$ , maximum tension developed in the geogrid increases because developed tension is  $J\varepsilon$  (where  $\varepsilon$  is the strain developed within the geogrid). Besides, increasing  $J$ , it will reduce the vertical stress in the soil above the geogrid, decreases the efficacy of the column. This is called the membrane action of the geogrid.

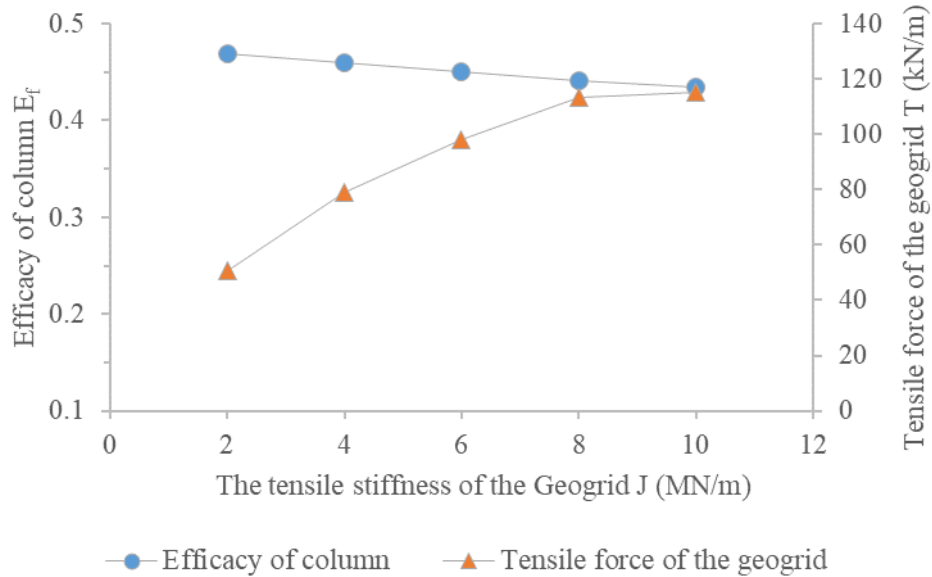


Figure 5. Influence of the tensile stiffness of the geogrid.

### 4. DISCUSSION

Two main factors affect the transmission efficiency to the columns ( $E_f$ ): the effective vertical load ( $\sigma_v'$ ) and ratio of the spacing of the columns and the column's diameter ( $s/D$ ). The efficacy of the column increases rapidly with an increase in effective vertical load from 0.23 to 0.44. In contrast, the efficacy decreases from 0.60 to 0.37 when  $s/D$  increased.

Fig. 2 to Fig. 5 show that the tensile force of the geogrid  $T$  in the analyzed cases increases with increasing the effective vertical load, ratio  $s/D$ , and the tensile stiffness of the geogrid  $J$ . When the ratio  $E_c/E_s > 150$  and  $J > 8000$  kN/m, the tensile force of the geogrid tends not to change much.

### 5. CONCLUSIONS

The result of this 3D numerical study demonstrates that the inclusion of geogrid in earth platforms can enhance the stress transfer from the soil to the columns. Analytical data indicated that two main factors affect the transmission efficiency to the columns: the effective vertical load and ratio of the spacing of the columns and the column's diameter.

In addition, an increase in the following factors will increase the tensile force of the geogrid including the effective vertical load, ratio  $s/D$ , and the tensile stiffness of the geogrid.

## REFERENCES

- [1]. J. Han, J. Huang, A. Porbaha, 2D numerical modeling of a constructed geosynthetic-reinforced embankment over deep mixed columns, *Contemporary issues in foundation engineering*, (2005) 1-11. [https://doi.org/10.1061/40777\(156\)13](https://doi.org/10.1061/40777(156)13)
- [2]. D. T. Bergado, P. V. Long, B.R. S. Murthy, A case study of geotextile-reinforced embankment on soft ground, *Geotextiles and Geomembranes*, 20 (2002) 343-365. [https://doi.org/10.1016/S0266-1144\(02\)00032-8](https://doi.org/10.1016/S0266-1144(02)00032-8)
- [3]. Standard, British, 8006-1 Code of practice for strengthened/reinforced soils and other fills, British Standards Institution, (2010).
- [4]. N. Yapage, Numerical modelling of geosynthetic reinforced embankments over soft ground improved with deep cement mixed columns, (2013). <http://handle.uws.edu.au:8081/1959.7/uws:31350>
- [5]. J. Han, M. A. Gabr, Numerical analysis of geosynthetic-reinforced and pile-supported earth platforms over soft soil, *Journal of geotechnical and geoenvironmental engineering*, 128 (2002) 44-53. [https://doi.org/10.1061/\(ASCE\)1090-0241\(2002\)128:1\(44\)](https://doi.org/10.1061/(ASCE)1090-0241(2002)128:1(44))
- [6]. S.J.M. Van Eekelen, A. Bezuijen, A. F. Van Tol, Analysis and modification of the British Standard BS8006 for the design of piled embankments, *Geotextiles and Geomembranes*, 29 (2011) 345-359. <https://doi.org/10.1016/j.geotexmem.2011.02.001>
- [7]. R. P. Chen et al., Tensile force of geogrids embedded in pile-supported reinforced embankment: A full-scale experimental study, *Geotextiles and Geomembranes*, 44 (2016) 157-169. <https://doi.org/10.1016/j.geotexmem.2015.08.001>
- [8]. Yapage, N. N. S., Liyanapathirana, D. S., Poulos, H. G., Kelly, R. B., & Leo, C. J, Numerical modeling of geotextile-reinforced embankments over deep cement mixed columns incorporating strain-softening behavior of columns, *International Journal of Geomechanics*, 15 (2015) 04014047. [https://doi.org/10.1061/\(ASCE\)GM.1943-5622.0000341](https://doi.org/10.1061/(ASCE)GM.1943-5622.0000341)
- [9]. J. Huang, J. Han, J. G. Collin, Geogrid-reinforced pile-supported railway embankments: A three-dimensional numerical analysis, *Transportation research record*, 1936 (2005) 221-229. <https://doi.org/10.1177/0361198105193600125>
- [10]. M. Bouassida, A. Porbaha, Ultimate bearing capacity of soft clays reinforced by a group of columns - Application to a deep mixing technique, *Soils and foundations*, 44 (2004) 91-101. [https://doi.org/10.3208/sandf.44.3\\_91](https://doi.org/10.3208/sandf.44.3_91)
- [11]. T. Himeno et al., Study on effects of specimen size of unconfined compressive strength of improved soil, *Lowland Technology International*, 20 (2019) 448-454. [http://cot.unhas.ac.id/journals/index.php/ialt\\_lti/article/view/604](http://cot.unhas.ac.id/journals/index.php/ialt_lti/article/view/604)